MIPA: A NEW MICRO-PATTERN DETECTOR*

P. Rehak, G.C. Smith, J.B. Warren and B. Yu
Brookhaven National Laboratory, Upton, NY 11973, USA

ABSTRACT

An anode-cathode array is being developed for electron multiplication in gas that lends itself to easy fabrication with lithographic techniques. Comprising an assembly of anode pins that are recessed into a closely-packed hexagonal cathode, the MIcro-Pin Array (MIPA) represents a promising addition to micro-pattern detectors with two-dimensional sensitivity. We describe the electrostatic rationale behind the MIPA detector's design, the fabrication technique, and X-ray results that illustrate electrical stability and high rate capability.

1 Introduction

A novel electron amplifying micro-structure is being developed for use as a position sensitive X-ray detector for dynamic crystallography at the National Synchrotron Light Source (NSLS) at Brookhaven National Laboratory. The energy of the X-rays, about 10 keV, is within the energy region where several centimeters of xenon at atmospheric pressure are sufficient to fully absorb the scattered radiation. The detector should provide a high resolution image of the diffraction patterns with an effective number of pixels of at least 1 million with the same resolution in both x and y directions. This implies that the relative position resolution should be better than one part in a thousand in each direction. Furthermore the total rate on the detector can approach 100 MHz.

The linear position resolution of the detector should be slightly smaller than the photon beam size, which is about 300 μm rms for current NSLS crystallography beam lines. It is very difficult to achieve these relative and absolute resolutions under such a high flux of incoming photons

*THIS RESEARCH WAS SUPPORTED BY THE U.S. DEPARTMENT OF ENERGY UNDER CONTRACT NO. DE-AC02-98CH10886.

using a global projective position encoding method, such as the standard wire chamber or MSGC technology.

However, the use of some form of "micro-pattern" gas amplification may be a suitable approach to achieve the required specifications, particularly if the complete detector is fabricated from smaller independent segments. In addition, the recently published method of decreasing parallax error[1] makes a xenon gas detector a suitable candidate for dynamic crystallography.

2 Stability of the Gas Amplification

To achieve the required longterm, stable performance under a high flux of radiation, the amplification region of a micro-pattern gas detector should at minimum satisfy the following two conditions:

1. No dielectric surface near the avalanche region.
2. First order stability of the field in the avalanche region with respect to electric discharge.

The importance of the first condition is well documented in the literature dealing with instabilities in most of the micro-pattern gas detectors[2], and is easy to understand. The charge on the surface of a dielectric depends on the previous history of the electric field and charges in the region above the surface. The presence of the charges on the surface influences the electric field in the amplification region leading to instabilities. Attempts to overcome this problem by using very high resistivity glasses or other layers have not been fully successful.[3]

The second condition concerns stability of gas amplification. In order to achieve the desirable gas gain in the amplification region, a set of suitable voltages are applied on the electrode structures of the gas detector. In the absence of any space charges within the gas of the detector, the geometry of the amplification region and the applied voltages define completely the electric field within the avalanche region. The amplification of the electrons in this region, filled with a particular gas mixture at a given pressure, depends only on the electric field. However, once the avalanche takes place, electrons are removed from this region much faster than the positive ions, modifying the electric field. If this modified electric field corresponds to one with higher gas gain, electrons arriving in the avalanche region produce even more charge and the combined effect can lead to a run-away phenomenon or an electric discharge. The condition of "first order stability" requires that the applied field in the charge free amplification region corresponds to a maximum of the gas gain. Any deviation from this field due to the presence of space charge should decrease the gas gain and prevent the amplification run-away.

Our analysis models the gas amplification according the classical work by Townsend. The avalanche process is described by the number of ionization collisions per unit length, called the first

Townsend coefficient, α. From this definition the natural logarithm of the gas gain is

$$\ln G = \int_{s_1}^{s_2} \alpha(U, U', s)\, ds, \tag{1}$$

where α can be a function of the voltage U and of the electric field $E = U'$ at a given point along the electron trajectory, s. s_1 and s_2 are the first and the last points on the trajectory of electrons within the avalanche region respectively. We will moreover assume that the potential at the first and the last point of this region are U_1 and U_2 respectively. The second requirement on the stability is thus reduced to a variational problem of finding a function $U(s)$ that maximizes the gas gain in Eq.1 with given values of voltages at both end points. ($U(s_1) = U_1$ and $U(s_2) = U_2$.)

The first Townsend coefficient α does not depend explicitly on the integration variable s, and the Euler equation

$$\frac{\partial \alpha}{\partial U} - \frac{d}{ds}\frac{\partial \alpha}{\partial U'} = 0 \tag{2}$$

gives the trivial solution $U' = (U_2 - U_1)/(s_2 - s_1) = \text{const}$. This is the case of a uniform field in a parallel plate geometry. However, for the values of α for our geometry the uniform field corresponds to the minimum rather than the maximum of the gain.

To obtain the function $U(s)$ that maximizes gain, the class of functions $U(s)$ in Eq.1 must be constrained to those satisfying the electrostatic conditions. We will follow a less general approach searching for a field in a particular form

$$E(r) = \frac{E_a \cdot r_a^n}{r^n}, \tag{3}$$

where we write explicitly the magnitude of the electric field $E(r)$ rather than U'. The parameter n, called the power of the field drop, describes the form of the field. $n = 0$ corresponds to a uniform field with 1 dimensional symmetry. $n = 1$ corresponds to the electric field around an anode wire with cylindrical symmetry. $n = 2$ corresponds to a field having spherical symmetry. The formula is exact with r_a being the radius of the anode wire. Other values of the parameter n have only a mathematical meaning.

Our initial tests have used a gas mixture of 80% Ar and 20% CO_2. The first Townsend coefficient, α, at atmospheric pressure can be parameterized as

$$\alpha(E) = a \cdot exp(-b/E), \tag{4}$$

where $a = 1.05/\mu\text{m}$ and $b = 13.25\, V/\mu\text{m}$.[4]

Figure 1 shows results of Eq.1 with electric field given by Eq.3, α being defined in Eq.4 for three different anode radii. We see that for practical values of anode radius around 20 μm, maximum gas gain is reached for $n \approx 1.7$. This power of the field drop is close to that of a spherical geometry. A practical detector geometry generating such a field is that of a pin with a semi-spherical tip of radius r_a, within a cylindrical cathode higher than the pin. Electric field simulations show that in such a structure, n does indeed vary from about 1.9 to 1.5.

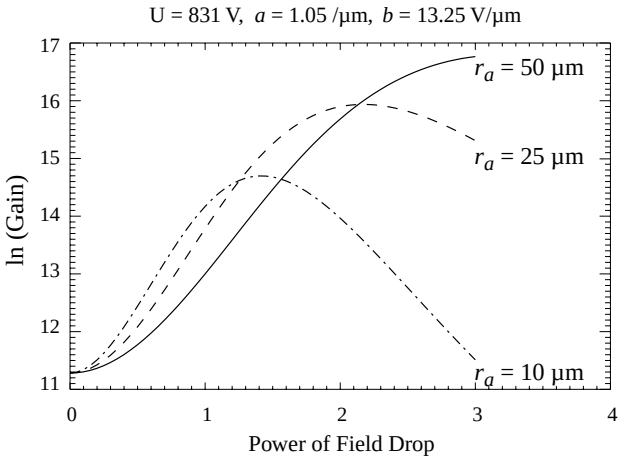

Figure 1: Natural logarithm of the gas gain as a function of the parameter n, called power of the field drop. The three curves correspond to different "anode radii" r_a. In all cases the radius of the cathode (extent of the field) is $r_c = r_a + 175\,\mu$m.

3 Prototype Electrodes

The MIPA electrodes were fabricated from SU-8, an epoxy-based, negative-acting photoresist that displays excellent transparency in the near UV. The relative UV transparency of this resist, when exposed with collimated UV radiation that minimizes lateral scattering, enables the fabrication of microstructures with vertical sidewalls and aspect ratios (sidewall height divided sidewall thickness) of 15:1. A standard chrome-on-quartz mask, typically used for lithography in integrated circuit fabrication, is used to fabricate the MIPA electrode array an SU-8 layer spun on to a silicon wafer.

Scanning electron micrographs in Figure 2 illustrates the primary fabrication steps. The anode, Figure 2a, is exposed with an initial mask to form an array of pins $50\,\mu$m in diameter and $200\,\mu$m high. After exposure and annealing, the SU-8 polymer cross-links and becomes insoluble in a developing solution that removes the unexposed material. The entire electrode array is then vacuum evaporated with gold. Then, an additional SU-8 layer is spun over the anode structure, and patterned with another mask consisting of a repeating hexagonal pattern. After development, the second SU-8 layer consists of a hexagonal honeycomb microstructure that forms the cathode, Figure 2b. Gold is vacuum deposited on the cathode, with the lower half of the structure being left uncoated to provide electrical isolation from the anode array. The full prototype consists of a 48×56 array of cells, each with an internal radius of $300\,\mu$m in the xy plane.

The position of the anode tips well below the upper plane of the cathode is the reason for the rapid change in electric field close to the tips. However, this recess may lead to a problem with full

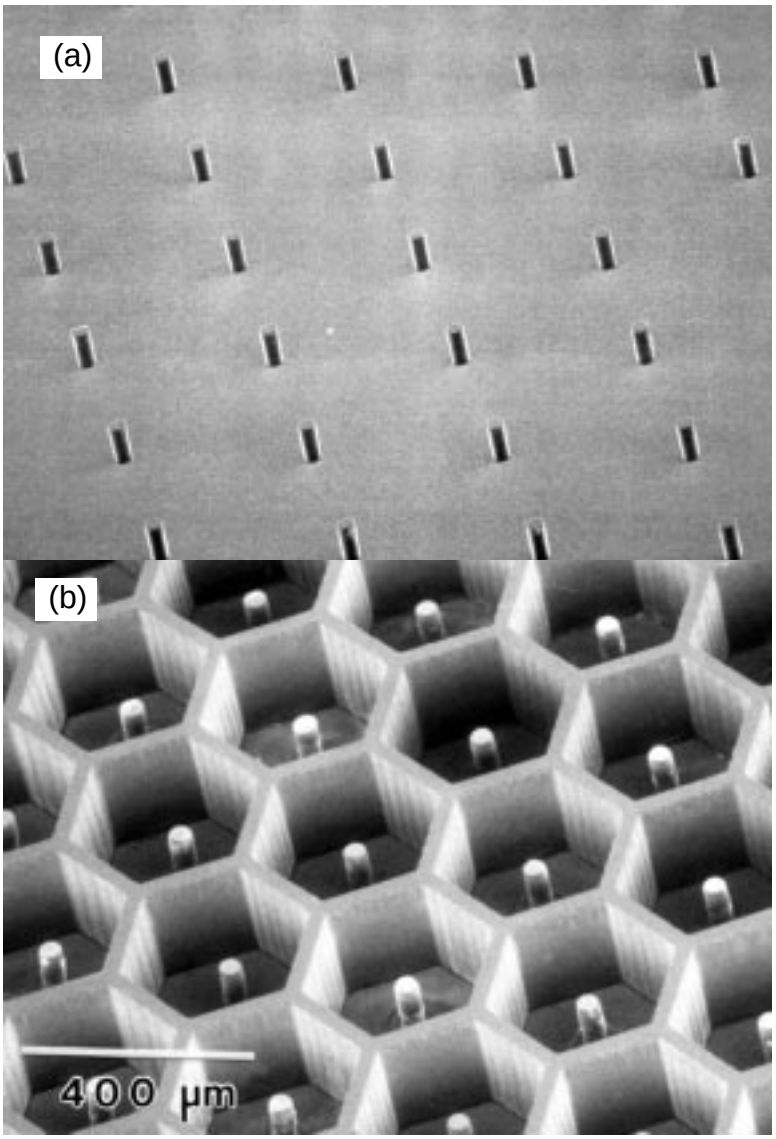

Figure 2: (a) Anode fabricated from SU-8, on silicon wafer; (b) Complete anode / cathode microstructure.

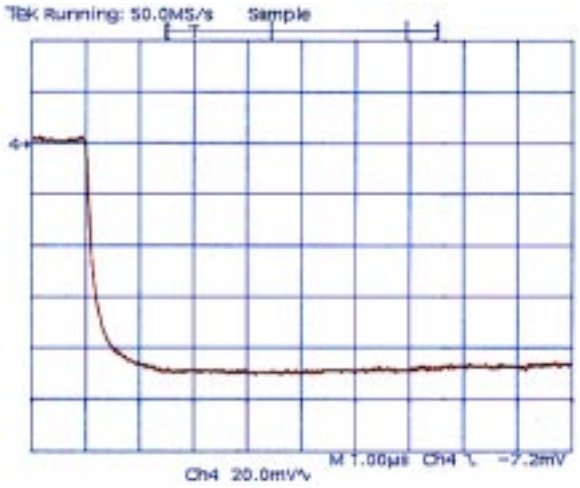

Figure 3: Signal waveform at the output of a charge sensing preamplifier connected to the cathode of the MIPA structure excited by a 5.9 keV X-ray.

collection of signal electrons produced by the X-rays in a drift volume directly above the cathode. All lines of force starting from the negatively biased window of the detector which encloses the drift volume must end on anodes, none of them on the cathode. A deeper recess of the anode tips inside the cathode structure requires a higher field in the amplification region relative to the field in the drift region. The recess chosen is a compromise between the sphericity of the amplification field (stability of operation) and full collection of electrons with a practical value of drift field. The hexagonal form of the individual cells minimizes the front surface of the cathode array as seen by signal electrons, thus improving electron collection properties of the array.

4 Experimental Results

The MIPA structure was enclosed in a box with an entrance window 1 cm above the cathode. For these initial tests all anodes were connected together and the cathode structure was left electrically undivided. A flow gas of 80% Ar and 20% CO_2 was used. The detector was operated with the cathode at ground potential, the anodes at a positive potential of several hundred volts, with the entrance window at a negative potential.

Figure 3 shows a signal waveform at the output of a charge sensing preamplifier connected to the cathode of the MIPA structure excited by 5.9 keV X-rays. An identical but inverted waveform was observed from an amplifier connected to the anodes. We see that the rise time of the integrated pulse, that is, the duration of the current signal, is about 1 μs. This corresponds to the drift time

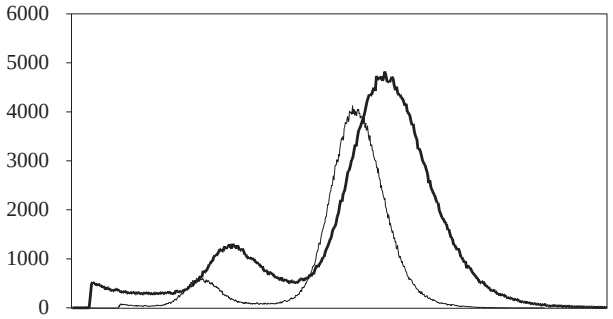

Figure 4: X-ray spectra from MIPA detector. Thin line: one or two cells illuminated by 5.4 keV X-rays. Thick line: entire prototype illuminated by 5.9 keV X-rays.

of the positive ions traversing the distance between the tip of the anode and the top plane of the cathode array.

Figure 4 shows X-rays spectra with a) only one or two cells illuminated and b) the entire array illuminated. We believe that the worsening of the energy resolution for full illumination of the detector is due to geometric imperfection of the array.

Figure 5 shows the dependence of gas gain on the anode voltage, measured with a charge sensing preamplifier followed by a 1 μs single delay line shaper. The detector can operate at a gain up to several times 10^4 without discharge.

The gas gain dependence has been studied as a function of photon rate using a collimated 5.4 keV X-ray beam. Figure 6 shows the results. At a nominal gas gain of 2400, a repeatable decrease in gain of about 10% for a rate of 10^6 X-rays $\mathrm{mm}^{-2}\mathrm{s}^{-1}$ was observed. This decrease may be due to the space charge, but is an acceptable decrease for most of the applications.

The geometry and the electric field of the amplification region of the MIPA detector are such that not all the positive ions created by the avalanche process return to the window. Figure 7 shows the ratio of current flowing to the entrance window (charge traversing the whole drift distance of the detector) to the current flowing to the cathode structure, as a function of the negative voltage applied to the window. The anode voltage was adjusted to maintain a constant gas gain. For small values of drift field, only about 5% of the positive ions created by avalanches return to the window. The ratio increases almost linearly with drift field. However, the drift time of positive ions within the drift region decreases with drift field. The net effect is that the density of positive charges in the drift region of the detector is, to first order, independent of drift field for constant flux and gas gain.

Figure 8 show the dependence of the 5.9 keV X-ray pulse height on the drift voltage for two different values of the gas gain. For values of drift voltage smaller than about 700 V (drift field below

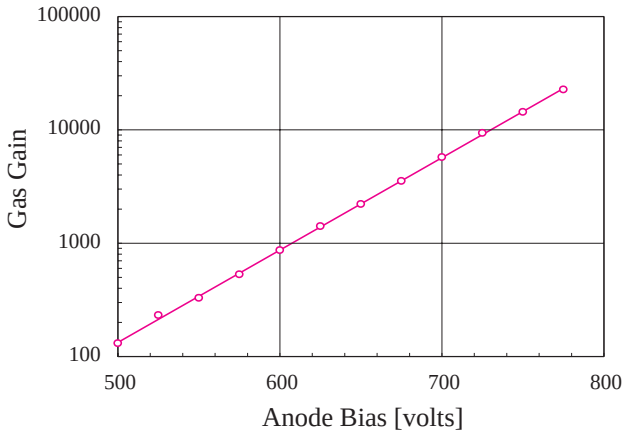

Figure 5: MIPA gas gain as a function of the anode pin bias voltage. (window at -500 V, 5.4 keV X-rays)

700 V/cm) the pulse height increases due to an increase in the electric field in the amplification region. However, a decrease in the pulse height is clearly visible once the negative voltage on the window exceeds 1000 V. The gas gain cannot decrease with higher values of electric field and our explanation is that a fraction of the primary electrons are being lost on the cathode structure of the MIPA. This hypothesis is supported by an observed worsening of the energy resolution for the higher value of drift field and also agrees with the field simulation.

5 Conclusions and Future Work

A new micro-structure for electron multiplication in gas is being developed, with the aim of overcoming electrical instabilities that have affected earlier micro-structure detectors. Initial experimental results indicate that characteristics specifically designed into the device to address this problem have succeeded.

Considerable work remains to be done. We are exploring methods to reduce geometric imperfections, fabricating structures that have anode pins with a smaller recess with respect to the top plane of the cathode, and improving our understanding of space charge effects. All these studies may improve gain uniformity. In the longer term, we are investigating methods to read-out position information either from groups of pins or from individual pins. We believe the MIPA represents a promising new detector that will have uses extending beyond its primary purpose in time-resolved X-ray crystallography.

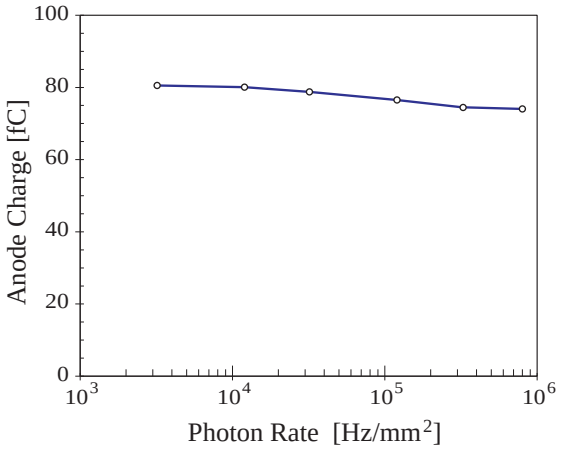

Figure 6: Anode charge as a function of photon rate with a collimated 5.4 keV X-ray beam. The beam size is $25\,\mu\text{m} \times 1\,\text{mm}$.

6 Acknowledgements

The authors wish to thank E.F. Von Achen and D.C. Elliott for assistance with the detector development.

References

[1] P. Rehak, G.C. Smith and B. Yu, "A Method for Reduction of Parallax Broadening in Gas-Based Position Sensitive Detectors," *IEEE Trans. Nucl. Sci.*, **44** (1997) 651-655

[2] A. Bressan et al, "High Rate Behavior and Discharge Limits in Micro-Pattern Detectors," *Nucl. Instrum. and Meth.* **A424** (1999)321-342

[3] C. Richter,"Microstrip-Gas-Chambers for the HERA-B Experiment," Proceedings of the International Workshop on Micro-Pattern Detectors, Orsay, France, June 28–30, 1999

[4] J.C. Armitage et al., "A Study of the Effect of Methane and Carbon Dioxide Concentration on Gas Amplification in Argon Based Gas Mixtures," *Nucl. Instrum. and Meth.*, **A271** (1988) 588-596

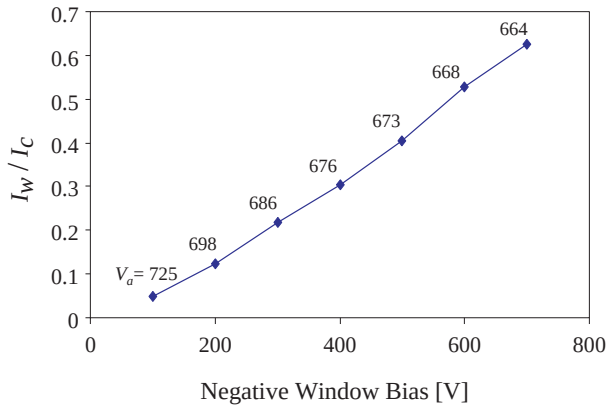

Figure 7: Ratio of current of positive ions returning to the entrance window and current of ions flowing into the cathode as a function of the negative window voltage.

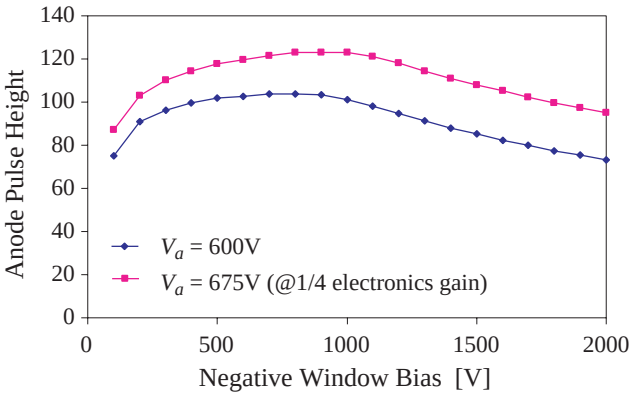

Figure 8: Pulse height of monochromatic X-rays as a function of the bias applied on the entrance window for two different anode voltages.